Carbohydrate Polymers 97 (2013) 581–586

Contents lists available at SciVerse ScienceDirect

Carbohydrate Polymers

journal homepage: www.elsevier.com/locate/carbpol

Short communication

Assessing cellulose microfibrillar structure changes due to cellulase action

Tina Jeoh*, Monica C. Santa-Maria[1], Patrick J. O'Dell

Department of Biological and Agricultural Engineering, University of California at Davis, Davis, CA 95616, United States

ARTICLE INFO

Article history:
Received 21 December 2012
Received in revised form 13 May 2013
Accepted 14 May 2013
Available online 21 May 2013

Keywords:
Trichoderma reesei Cel7A
Cellobiohydrolase
Cellulose microfibrils
Fibrillation
AFM

ABSTRACT

There is a need to understand how cellulose structural properties impact productive cellulase–cellulose interactions toward solving the mechanisms of the heterogeneous reaction. We coupled biochemical studies of cellulose hydrolysis by a purified *Trichoderma reesei* Cel7A (TrCel7A) cellobiohydrolase with atomic force microscopy (AFM) to study the impact of the cellulolytic activity on the fibrillar structure of cellulose. Bacterial cellulose (BC) fibrils were hydrolyzed by TrCel7A then immobilized by hydrophobic interactions on glass for AFM imaging. Commonly used methods to culture and isolate cellulose fibrils resulted in significant oxidation of the reducing-ends but minimal oxidation along the fibrils. We observed extensive fibrillation of BC fibrils to ~3 nm microfibrils during the course of hydrolysis by TrCel7A, leaving thinned un-fibrillated recalcitrant fibrils at >80% hydrolysis extents. Additionally, this remaining fraction appeared to be segmented along the fibril length.

1. Introduction

Cellulose is of industrial importance as a renewable resource for conversion to biofuels, biochemicals (Foust, Aden, Dutta, & Phillips, 2009; Himmel et al., 2007) and as functional components in advanced materials (Lahiji, Boluk, & McDermott, 2012; Lu & Hsieh, 2010). Due to its natural recalcitrance, one of the biggest technological challenges to realizing a cellulosic bioproducts industry lies in engineering inexpensive strategies to depolymerize cellulose.

A persistent mystery surrounding cellulase hydrolysis of cellulose is the characteristic decline in hydrolysis rates over the course of the reaction. In studies using purified *Trichoderma reesei* Cel7A (TrCel7A), a reducing-end specific cellobiohydrolase, it was shown that the hydrolysis rate decline tracks with a decline in the apparent catalytic rate constant (Jalak, Kurašhin, Teugjas, & Väljamäe, 2012; Kurasin & Valjamae, 2011). Substrate properties have been speculated to be the limiting factor (Cruys-Bagger, Elmerdahl, & Praestgaard, 2012; Kurasin & Valjamae, 2011; Zhang, Wolfgang, & Wilson, 1999), but understanding is limited. Native cellulose microfibrils are linear cellulose polymers associated via extensive hydrogen bonding and hydrophobic stacking interactions to organize into crystalline lattices that exclude water (Nishiyama, Langan, & Chanzy, 2002; Nishiyama, Sugiyama, Chanzy, & Langan, 2003). Microfibrils associate into larger fibrils (White & Brown, 1981) resulting in insoluble fibrillar structures where only celluloses on the outer surfaces are accessible to hydrolysis at the solid/aqueous interface by soluble cellulolytic enzymes. Cellulose fibrils undergo macroscopic changes in the supramolecular organization (Chanzy, Henrissat, Vuong, & Schulein, 1983; Santa-Maria & Jeoh, 2010; White & Brown, 1981) and nano-scale changes in surface properties (Wang et al., 2012) due to cellulolytic action.

Here we present details of methods to characterize and immobilize cellulose fibrils to facilitate biochemical and imaging studies of cellulose fibrillar properties. With these methods, we present results showing changes in the microstructure of cellulose fibrils due to the action of a purified TrCel7A.

2. Materials and methods

2.1. Preparation of cellulose fibrils

Pellicles from *Gluconacetobacter xylinus* (ATCC 700178) cultures (Santa-Maria & Jeoh, 2010) were rinsed, then washed in 1% sodium hydroxide (4 °C, 12 h, shaking at 60 rpm) and 0.3% sodium hypochlorite (pH 4.9 adjusted with glacial acetic acid, 2 h, 70 °C, gentle agitation) and repeated as necessary. The pellicles were rinsed until the conductivity reached 0.5–5 μS/cm and stored with 0.02% sodium azide at 4 °C.

Microfibrils (4 mL of ~0.5 mg/mL) were dispersed by ultrasonication with a 1/8 in microtip (Misonix Ultrasonicator S-4000, Qsonica, LLC, Newtown, CT) at 30% amplitude and 2× 15-s pulses (220–283 J).

* Corresponding author. Tel.: +1 530 752 1020; fax: +1 530 752 2460.
E-mail address: tjeoh@ucdavis.edu (T. Jeoh).
[1] Present address: Global Alimentos S.A.C., Sevilla 244, Lima 18, Peru.

0144-8617/$ – see front matter © 2013 Elsevier Ltd. All rights reserved.
http://dx.doi.org/10.1016/j.carbpol.2013.05.027

Cellulose reducing end concentrations were estimated by the bicinchoninic assay (BCA) (Doner & Irwin, 1992). Carbon, hydrogen and nitrogen (CHN) contents of lyophilized BC were analyzed using air and a barley standard (1.69% N) as calibrants (TruSpec CHN analyzer, LECO Corp., St. Joseph, MI).

2.2. Measuring oxidized groups on cellulose

The carboxyl content of cellulose was measured by conductimetry (Habibi, Chanzy, & Vignon, 2006). The conductivity of cellulose suspensions (1–3 mg/mL in 40 mL) in 0.1 mM NaCl and 2 mL of 10 mM HCl was recorded (InLab® 731 conductivity probe, Mettler Toledo, Schwerzenbach, CH), then titrated with 10 mM NaOH. The concentration of carboxyl groups is equivalent to the moles of NaOH added in the nonlinear range of the titration curve (Supplementary information 1). The carboxyl content of cellulose is reported as mmole —COOH/mole glucose measured by the Anthrone assay using glucose as the standard (Morris, 1948).

Aldehyde groups on cellulose were selectively oxidized to carboxylic acids by reacting 150 mg of cellulose in 50 mL of sodium acetate buffer (pH 4) and 300 mg of sodium chlorite ($NaClO_2$) for 40 h at room temperature (RT). The ketone groups on ~0.1 mg/mL of $NaClO_2$ treated cellulose was reacted with 0.01 mg/mL Alexa Fluor 488-hydrazine (AF488-Hyd) (Life Technologies, Grand Island, NY) in 200 mM sodium acetate buffer pH 5.0 and shaken at 200 rpm overnight at RT. AF488-cellulose was filtered (0.2 μm, 25 mm dia, Isopore™, MilliPore), washed, then resuspended in sodium acetate buffer. Fluorescence intensities at E_x/E_m 488/520 nm were converted to concentrations using an AF488-Hyd standard curve. The ketone content of cellulose is reported as μmole ketone/mole glucose.

2.3. Hydrolysis of BC by TrCel7A

TrCel7A was purified from Celluclast (Novozymes, Inc.) and labeled with Alexa Fluor 594 (Life Technologies, Grand Island, NY) (AF594TrCel7A) (Santa-Maria & Jeoh, 2010).

Dispersed BC was combined with 10 μmole AF594TrCel7A/g cellulose in 0.5 mL total volume, 50 mM sodium acetate pH 5.0 and rotated end-over-end at RT in the dark. Substrate-only and enzyme-only controls were prepared in parallel. All reaction components were equilibrated to RT for >30 min before the reactions were

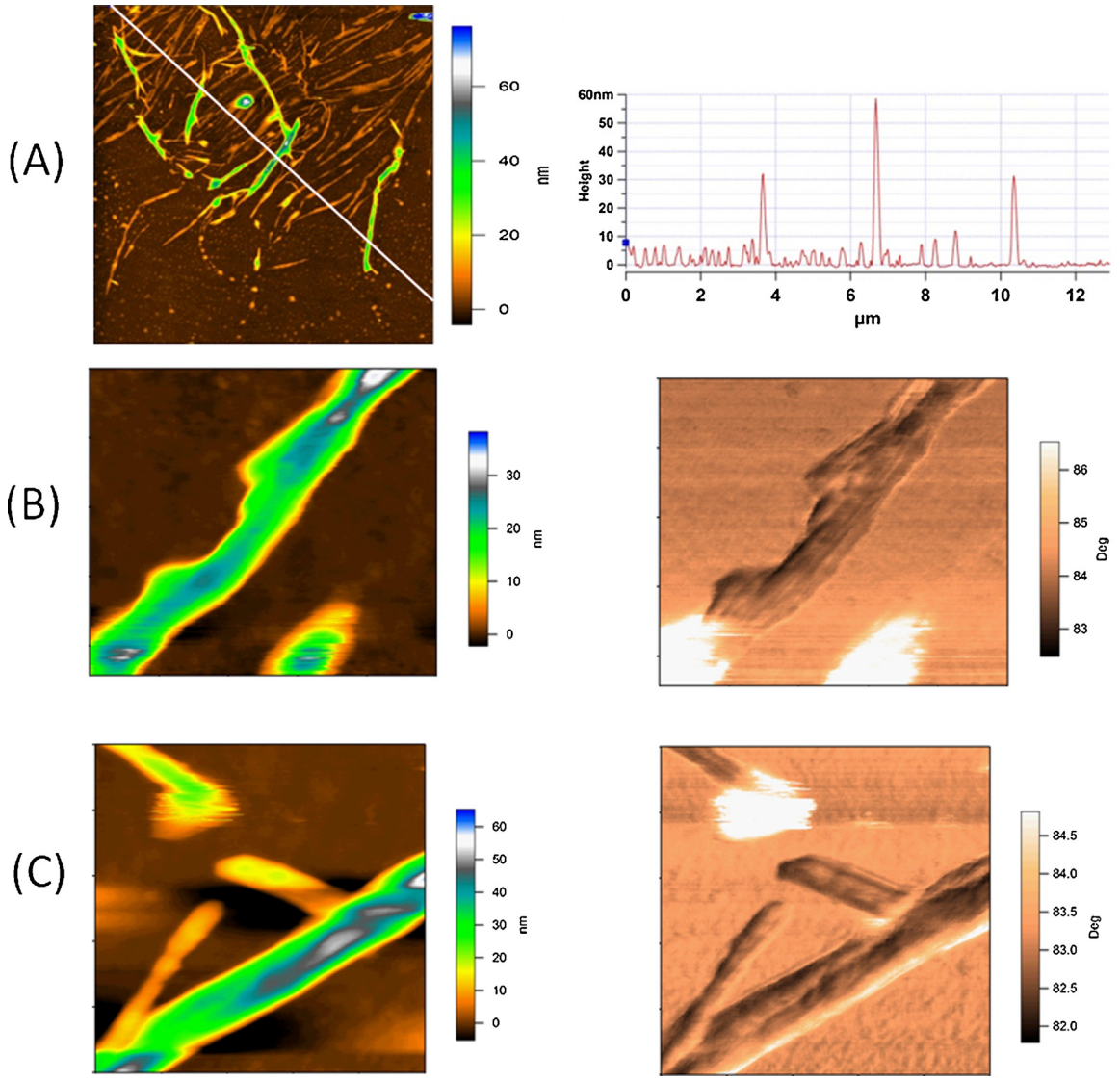

Fig. 1. ABA washed BC fibrils immobilized on glass. These images correspond to the substrate-only control and zero time point in the hydrolysis experiments. (A) 10 μm × 10 μm field of view (FOV) (dimensions of the image shown). Left: AFM height image, right: cross-section height profile corresponding to the white line in the height image; (B and C) 1 μm × 1 μm FOV. Left: height data, right: phase data.

initiated by adding AF594TrCel7A. Of five replicates, three were terminated by filtering in 0.45 μm filters (AcroPrep, Supor membrane, Pall Corporation, Ann Arbor, MI). The filtrate was analyzed for solubilized sugars (Dionex IC-5000, Carbopac SA10, 10 mM sodium hydroxide, Thermo Scientific, Sunnyvale, CA) and the retentate was resuspended in 250 μl of buffer and measured at E_x/E_m 594/620 to determine concentrations of TrCel7A bound to cellulose (Davis, Wolfrum, & Jeoh, 2008). Two replicates were boiled for 15 min, combined and imaged by AFM. Neither boiling nor sonication caused microfibrillar changes observed with enzyme action (Fig. 1). Only cellobiose was detected in all samples, while no soluble sugars were detected in the controls.

2.4. AFM imaging of cellulose fibrils

RCA1 cleaned glass coverslips (No. 1, 25 mm dia., Fisher Scientific) were silanized with methyltrimethoxyl silane (MTMS) (Gelest, Inc.) by anhydrous vapor deposition (at <20 Torr for 24 h) and stored under argon (Dong, Wang, Simon Ng, Mao, & 2006; Santa-Maria & Jeoh, 2010). Average contact angles of water on MTMS-glass, unsilanized glass and aminopropyltriethoxysilane (APTES)-glass were 66°, 49° and 16°, respectively.

Microfibrils were adhered to the silanized glass by sedimenting a suspension (1.5–2 mL) on the glass at 453 × *g* for 15 min in a swinging bucket rotor. The cover slips were assembled into fluid cell clamps (Asylum research, parts no. 111.789 and 111.790) then rinsed to remove unattached microfibrils. Water was kept on the surface at all times.

Tapping mode AFM was conducted in fluid with silicon tips (AC240TS cantilever, 2 N/m; Asylum Research) using a MFP3D BIO AFM system (Asylum Research) (Santa-Maria & Jeoh, 2010). Cantilevers were tuned to −5% of 1 V free amplitude. Typical scan rate was 0.5–1 Hz with 512 × 512 scan points × lines. Images were flattened and analyzed using IGOR Pro 6.12 (Wavemetrics), but not corrected for tip broadening or drift.

3. Results and discussion

3.1. Isolation and oxidation of cellulose

Multiple washes in dilute alkali and bleach were necessary to completely isolate cellulose. Of primary concern was the presence of protein, determined by CHN analysis (Table 1). The minimum processing required to remove all traces of N from BC was a sequence of alkali, bleach and alkali (ABA) washes. Nitrogen-free BC samples dispersed easily with milder sonication (30 s at 30% of maximum intensity) than was previously necessary (~1 h at maximum intensity) (Santa-Maria & Jeoh, 2010).

The secondary alcohols at C2, C3 and C4 (non-reducing end), the primary alcohol of the hydroxymethyl group (C6) and the aldehyde of the reducing end (C1) can oxidize to ketone, aldehydes and carboxylic acid groups, respectively (Lewin & Epstein, 1962) (Supplementary information 2). The hydroxymethyl groups of cellulose are the most resistant to oxidation (Xu, Ding, & Tejirian, 2009), and hypochlorite selectively oxidizes secondary alcohols with little activity on primary alcohols (Isogai, Saito, & Fukuzumi, 2011; Saito & Isogai, 2004; Stevens, Chapman, & Weller, 1980). Thus we attribute all aldehyde groups in the cellulose samples to native reducing-ends, and not as products of oxidation of the (C6) hydroxymethyl group. ABA washed BC had 5.5 ± 1.1 mmole reducing groups/mole glucose and 2.6 ± 1.4 mmole —COOH/mole glucose. The total reducing end content of the BC was 8.1 mmole reducing ends/mole glucose, with ~32% oxidized. The ketone content of ABA washed BC was 10 ± 2 μmole ketone/mole glucose indicating that on average, every ~100,000 glucose residue contained an oxidized C2, C3 (or C4) group.

Table 1
Nitrogen content of bacterial cellulose processed by alkali and bleach washing steps.

Wash sequence[a]	Nitrogen content (% db)
A	1.4
AB	0.87
ABA	ND[b]
ABAB	ND[b]

[a] A, alkali wash; B, bleach wash: the order of the letters indicate the order of the wash steps.
[b] ND, not detected.

3.2. Adhesion of cellulose fibrils to glass

Cellulose fibrils of a range of size and lengths were immobilized by hydrophobic interactions on methylated glass (Fig. 1A). Thinner microfibrils (3–5 nm height) were more weakly adhered and more susceptible to movement or displacement by the AFM tip (e.g. in Figs. 3B and 4B) while thicker fibrils were immobile over repeated scans. Gas/air bubbles were occasionally observed at the hydrophobic surface (Ishida, Inoue, Miyahara, & Higashitani, 2000) resulting in areas of increased phase lag (brighter regions) in the phase images (Fig. 1B and C).

3.3. Hydrolysis and fibrillation of cellulose fibrils

The extent of BC hydrolysis by TrCel7A reached up to 91.5% (std. dev. 2.5%) in 48 h (Fig. 2A). The hydrolysis profile suggests three regimes: rapid initial hydrolysis of ~40% of the cellulose, nearly linear increase between 45 and 80% hydrolysis and a noticeable decline in rate by 91% hydrolysis. The initial BC sample (Fig. 1A) contained a noticeable fraction of thin (≤5 nm) fibrils amongst thicker

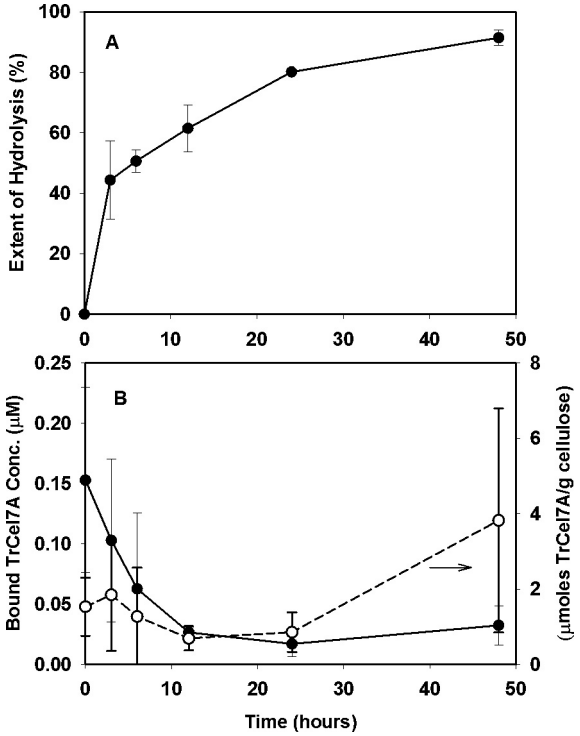

Fig. 2. TrCel7A hydrolysis of BC (10 μmole AF594TrCel7A/g cellulose loading) at pH 5 and 21 °C. (A) extent of hydrolysis, and (B) bound enzyme concentrations in solution concentrations and per gram of remaining cellulose (filled circles in μM bound enzymes (primary *y*-axis) while open circles in μmole bound enzyme/g remaining cellulose (secondary *y*-axis)). Lines drawn to guide the eye.

fibrils (~30–60 nm) not observed in more extensively hydrolyzed samples. At higher resolution, the thick BC fibrils appear generally intact with some contrasts in the phase images suggesting multiple thinner microfibrils tightly associated into the larger fibrils (Fig. 1B and C).

Between ~45 and 80% hydrolysis, most of the fibrils appeared as bundles of thinner microfibrils (3–5 nm) that were fibrillating at various sections along the lengths (Fig. 3 and Supplementary information 3). This confirms similar observations made with TrCel7A hydrolysis of [5-(4,6-dichlorotriazinyl)aminofluorescein] (DTAF)-labeled BC (Santa-Maria & Jeoh, 2010). White and Brown (1981) reported 'splaying' of BC ribbons into ~3–3.5 nm microfibrils by the action of *T. reesei* cellulases. Fibrillation of algal cellulose from *Valonia* spp. due to Cel7A action (Chanzy et al., 1983; Imai, Boisset, Samejima, Igarashi, & Sugiyama, 1998) and cellulose fibrils in the cell wall of corn roots by cellulases (Mueller & Brown, 1980) have also been reported. One might intuit that separation of larger fibrils into thin ~3 nm microfibrils increases accessible surface area for enzymatic action. Yet, between 45 and 80% hydrolysis where fibrillation was commonly observed, the bound enzyme/remaining cellulose ratio and hydrolysis rates declined (Fig. 2).

3.4. Thinning and segmentation of cellulose fibrils

Cellulose fibrils at 91.5% hydrolysis did not have the appearance of fibrillating assemblies. Rather, the fibrils were thin (~2–6 nm)

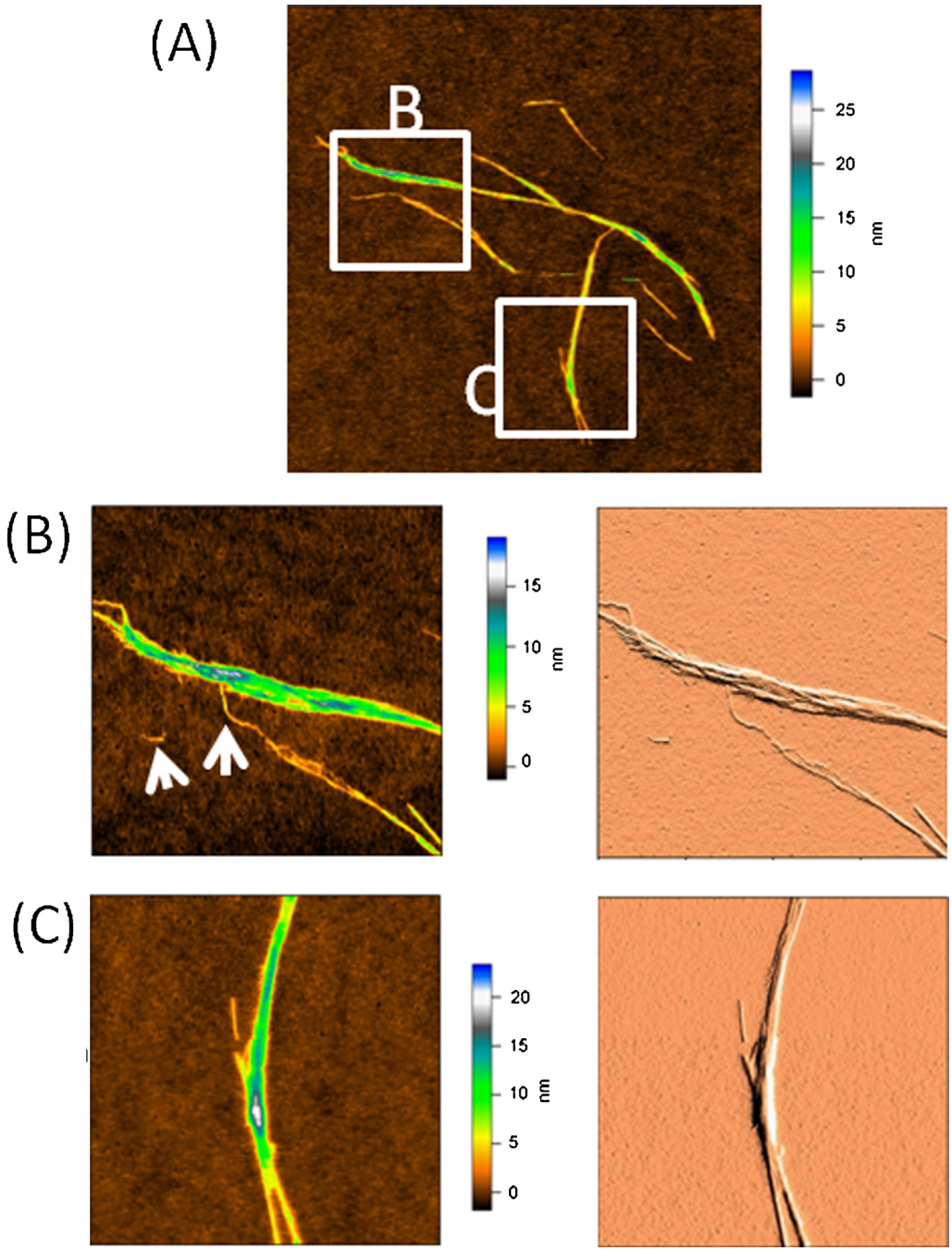

Fig. 3. One example of a fibrillating BC fibril observed at 24 h (80.2% hydrolysis). (A) AFM height image (7 μm × 7 μm FOV). White boxes correspond to higher resolution scans in (B) and (C). (B and C) 2 μm × 2 μm FOV. Left: AFM height data, right: amplitude data. The arrows in B point to a microfibril that moved during scanning. Additional examples are shown in Supplementary information 3.

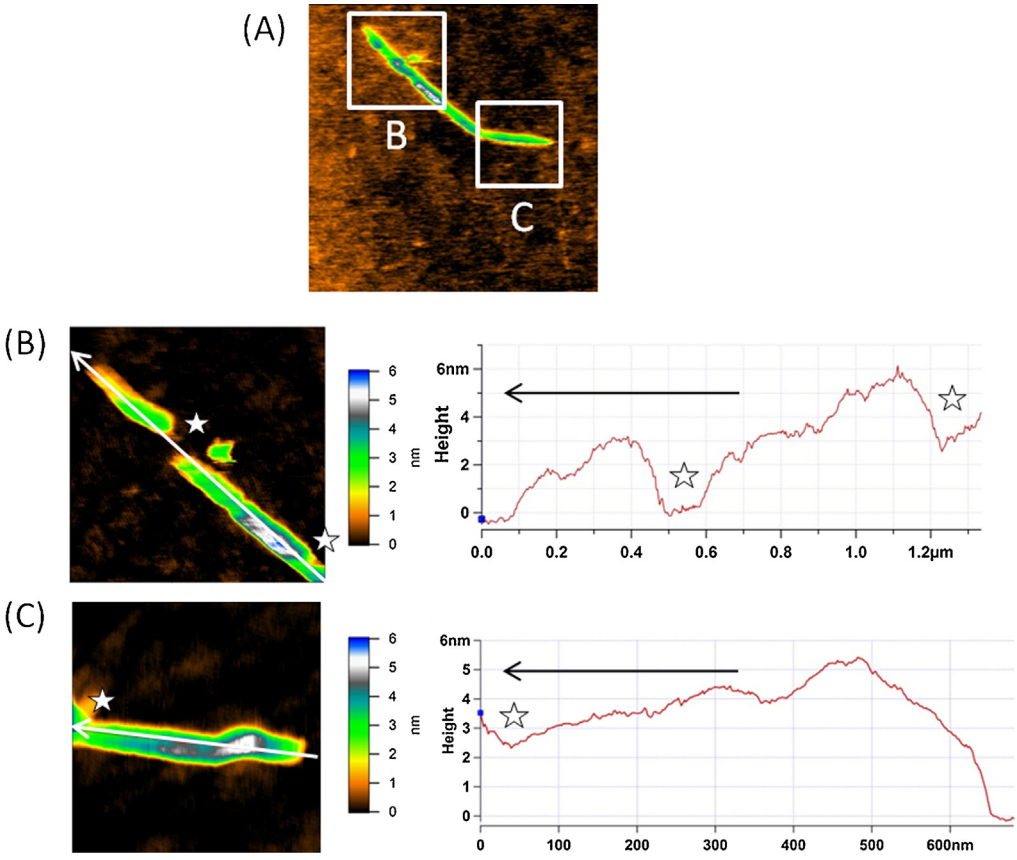

Fig. 4. One example of thinned and segmented BC fibril observed at 48 h (A) AFM height data (3 μm × 3 μm FOV). White boxes correspond to higher resolution scans in (B) and (C). (B) AFM height data (1 μm × 1 μm FOV) and (C) (0.7 μm × 0.7 μm FOV). In (B and C), left: AFM height data, right: cross-section height profile corresponding to the arrow in the height image. Arrow direction in the height images corresponds to those in the cross section graphs. Stars indicate locations where segmentation of the fibril was observed. Additional examples are shown in Supplementary Information 4.

with preferential thinning at one end of the fibrils (Fig. 4 and Supplementary information 4). Some of the fibrils appeared to be severing along the lengths into shorter, ~0.5 μm segments that are also thinned at one end (Fig. 4B and C). Thinned fibrils were more weakly attached to the surface. Fig. 4B shows a 1 μm × 1 μm scan of one end of the fibril shown in Fig. 4A where a separated segment is evident only in the higher resolution scan as it moved during multiple scans of the same area. Cellulose fibril segmentation was previously observed on *Valonia* cellulose hydrolyzed by *T. reesei* Cel6A (CBHII) and Cel5A (EGII) likely due to endo-activity (Chanzy & Henrissat, 1985). In another case, segmentation with preferential thinning of the reducing end was observed on *Valonia* microcrystals hydrolyzed by purified TrCel7A (Imai et al., 1998) leading the authors to speculate possible endo-activity of TrCel7A or trace amounts of endocellulase. TrCel7A in the current study was affinity purified over a *p*-aminophenyl cellobioside (*p*APC) matrix demonstrated to effectively separate endocellulases (Sangseethong & Penner, 1998). Thus the segmentation of the fibrils is unlikely due to endocellulase contamination. Further investigation into BC fibril properties and *T. reesei* Cel7A mode of action is necessary to elucidate the reason for the segmentation.

4. Conclusions

Bacterial cellulose fibrils were produced and isolated by commonly used methods and found that oxidation was extensive (~32%) at the reducing ends but limited along the lengths. Cellulose fibrils were successfully immobilized to hydrophobized glass in buffer, establishing a method for AFM visualization of never-dried and minimally modified cellulose. Further work is needed to minimize processing impacts on cellulose surface chemistry to allow experiments with pristine fibrils. Hydrolysis with TrCel7A confirmed previous observations with DTAF-BC that cellobiohydrolase activity fibrillates larger bundles, leaving a recalcitrant, unfibrillated, but thinned fraction. We further observed segmentation of the fibrils, an unexpected outcome for a reducing-end specific cellobiohydrolase.

Acknowledgements

The authors thank Dr. Chao-Wei Yu for assistance with the CHN analyses of cellulose, Scott Strobel for contributions toward the development of methods for measuring cellulose oxidation, and Alan Hicklin and the Keck Spectral Imaging Facility (KSIF) of UC Davis for technical support and use of the AFM. This publication is based on work supported by the National Science Foundation CBET (Grant No. 1055518), IGERT (Grant No. DGE-0653984), and REU programs (Grant No. 0852090).

Appendix A. Supplementary data

Supplementary data associated with this article can be found, in the online version, at http://dx.doi.org/10.1016/j.carbpol.2013.05.027.

References

Chanzy, H., & Henrissat, B. (1985). Undirectional degradation of *Valonia* cellulose microcrystals subjected to cellulase action. *FEBS Letters*, *184*(2), 285–288.

Chanzy, H., Henrissat, B., Vuong, R., & Schulein, M. (1983). The action of 1,4-beta-D-glucan cellobiohydrolase on *Valonia* cellulose microcrystals: An electron microscopic study. *FEBS Letters*, *153*(1), 113–118. http://dx.doi.org/10.1016/0014-5793(83)80129-x

Cruys-Bagger, N., Elmerdahl, J., & Praestgaard, E. (2012). Pre-steady-state kinetics for hydrolysis of insoluble cellulose by cellobiohydrolase Cel7A. *Journal of Biological Chemistry*, *287*(22), 18451–18458. http://dx.doi.org/10.1074/jbc.M111.334946

Davis, M. F., Wolfrum, E., & Jeoh, T. (2008). Selection of promising biomass feedstock lines using high-throughput spectrometric and enzymatic assays. In W. Vermerris (Ed.), *Genetic improvement of bioenergy crops*. New York, NY: Spring Science + Business Media, LLC.

Doner, L. W., & Irwin, P. L. (1992). Assay of reducing end-groups in oligosaccharide homologs with 2,2′-bicinchoninate. *Analytical Biochemistry*, *202*(1), 50–53.

Dong, J., Wang, A., Simon Ng, K. Y., & Mao, G. (2006). Self-assembly of octadecyltrichlorosilane monolayers on silicon-based substrates by chemical vapor deposition. *Thin Solid Films*, *515*(4), 2116–2122.

Foust, T. D., Aden, A., Dutta, A., & Phillips, S. (2009). An economic and environmental comparison of a biochemical and a thermochemical lignocellulosic ethanol conversion process. *Cellulose*, *16*, 547–565.

Habibi, Y., Chanzy, H., & Vignon, M. R. (2006). TEMPO-mediated surface oxidation of cellulose whiskers. *Cellulose*, *13*(6), 679–687. http://dx.doi.org/10.1007/s10570-006-9075-y

Himmel, M. E., Ding, S. Y., Johnson, D. K., Adney, W. S., Nimlos, M. R., & Brady, J. W. (2007). Biomass recalcitrance: Engineering plants and enzymes for biofuels production. *Science*, *315*(5813), 804–807. http://dx.doi.org/10.1126/science.1137016

Imai, T., Boisset, C., Samejima, M., Igarashi, K., & Sugiyama, J. (1998). Unidirectional processive action of cellobiohydrolase Cel7A on *Valonia* cellulose microcrystals. *FEBS Letters*, *432*, 113–116.

Ishida, N., Inoue, T., Miyahara, M., & Higashitani, K. (2000). Nano bubbles on a hydrophobic surface in water observed by tapping-mode atomic force microscopy. *Langmuir*, *16*(16), 6377–6380. http://dx.doi.org/10.1021/la000219r

Isogai, A., Saito, T., & Fukuzumi, H. (2011). TEMPO-oxidized cellulose nanofibers. *Nanoscale*, *3*(1), 71–85. http://dx.doi.org/10.1039/c0nr00583e

Jalak, J., Kurašhin, M., Teugjas, H., & Väljamäe, P. (2012). Endo–exo synergism in cellulose hydrolysis revisited. *Journal of Biological Chemistry*, http://dx.doi.org/10.1074/jbc.M112.381624

Kurasin, M., & Valjamae, P. (2011). Processivity of cellobiohydrolases is limited by the substrate. *Journal of Biological Chemistry*, *286*(1), 169–177. http://dx.doi.org/10.1074/jbc.M110.161059

Lahiji, R. R., Boluk, Y., & McDermott, M. (2012). Adhesive surface interactions of cellulose nanocrystals from different sources. *Journal of Materials Science*, *47*(9), 3961–3970. http://dx.doi.org/10.1007/s10853-012-6247-z

Lewin, M., & Epstein, J. A. (1962). Functional groups and degradation of cotton oxidized by hypochlorite. *Journal of Polymer Science*, *58*(166), 1023.

Lu, P., & Hsieh, Y.-L. (2010). Preparation and properties of cellulose nanocrystals: Rods, spheres, and network. *Carbohydrate Polymers*, *82*(2), 329–336.

Morris, D. L. (1948). Quantitative determination of carbohydrates with dreywoods anthrone reagent. *Science*, *107*(2775), 254–255.

Mueller, S. C., & Brown, R. M. (1980). Evidence for an intramembrane component associated with a cellulose microfibril-synthesizing complex in higher plants. *Journal of Cell Biology*, *84*(2), 315–326. http://dx.doi.org/10.1083/jcb.84.2.315

Nishiyama, Y., Langan, P., & Chanzy, H. (2002). Crystal structure and hydrogen-bonding system in cellulose I-beta from synchrotron X-ray and neutron fiber diffraction. *Journal of the American Chemical Society*, *124*, 9074–9082.

Nishiyama, Y., Sugiyama, J., Chanzy, H., & Langan, P. (2003). Crystal structure and hydrogen bonding system in cellulose 1(alpha), from synchrotron X-ray and neutron fiber diffraction. *Journal of the American Chemical Society*, *125*(47), 14300–14306. http://dx.doi.org/10.1021/ja037055w

Saito, T., & Isogai, A. (2004). TEMPO-mediated oxidation of native cellulose. The effect of oxidation conditions on chemical and crystal structures of the water-insoluble fractions. *Biomacromolecules*, *5*(5), 1983–1989. http://dx.doi.org/10.1021/bm0497769

Sangseethong, K., & Penner, M. H. (1998). p-Aminophenyl beta-cellobioside as an affinity ligand for exo-type cellulases. *Carbohydrate Research*, *314*(3), 245–250.

Santa-Maria, M., & Jeoh, T. (2010). Molecular-scale investigations of cellulose microstructure during enzymatic hydrolysis. *Biomacromolecules*, *11*(8), 2000–2007. http://dx.doi.org/10.1021/bm100366h

Stevens, R. V., Chapman, K. T., & Weller, H. N. (1980). Convenient and inexpensive procedure for oxidation of secondary alcohols to ketones. *Journal of Organic Chemistry*, *45*(10), 2030–2032. http://dx.doi.org/10.1021/jo01298a066

Wang, J. P., Quirk, A., Lipkowski, J., Dutcher, J. R., Hill, C., & Mark, A. (2012). Real-time observation of the swelling and hydrolysis of a single crystalline cellulose fiber catalyzed by cellulase 7B from *Trichoderma reesei*. *Langmuir*, *28*(25), 9664–9672. http://dx.doi.org/10.1021/la301030f

White, A. R., & Brown, R. M. (1981). Enzymatic hydrolysis of cellulose: Visual characterization of the process. *Proceedings of the National Academy of Sciences of the United States of America: Biological Sciences*, *78*(2), 1047–1051. http://dx.doi.org/10.1073/pnas.78.2.1047

Xu, F., Ding, H., & Tejirian, A. (2009). Detrimental effect of cellulose oxidation on cellulose hydrolysis by cellulase. *Enzyme and Microbial Technology*, *45*(3), 203–209. http://dx.doi.org/10.1016/j.enzmictec.2009.06.002

Zhang, S., Wolfgang, D. E., & Wilson, D. B. (1999). Substrate heterogeneity causes the nonlinear kinetics of insoluble cellulose hydrolysis. *Biotechnology and Bioengineering*, *66*(1), 35–41.